




Increases in hypertension-induced cerebral microhemorrhages exacerbate gait dysfunction in a mouse model of Alzheimer's disease

Ádám Nyúl-Tóth · Stefano Tarantini · Tamas Kiss · Peter Toth · Veronica Galvan · Amber Tarantini · Andriy Yabluchanskiy · Anna Csiszar · Zoltan Ungvari 

Received: 19 May 2020 / Accepted: 17 August 2020 / Published online: 25 August 2020
© American Aging Association 2020

Abstract Clinical studies show that cerebral amyloid angiopathy (CAA) associated with Alzheimer's disease (AD) and arterial hypertension are independent risk factors for cerebral microhemorrhages (CMHs). To test the hypothesis that amyloid pathology and hypertension interact to promote the development of CMHs, we

induced hypertension in the Tg2576 mouse model of AD and respective controls by treatment with angiotensin II (Ang II) and the NO synthesis inhibitor L-NAME. The number, size, localization, and neurological consequences (gait alterations) of CMHs were compared. We found that compared to control mice, in TG2576 mice,

Ádám Nyúl-Tóth, Stefano Tarantini and Andriy Yabluchanskiy contributed equally to this work.

Á. Nyúl-Tóth · S. Tarantini · T. Kiss · P. Toth · A. Tarantini · A. Yabluchanskiy · A. Csiszar · Z. Ungvari
Vascular Cognitive Impairment and Neurodegeneration Program, Reynolds Oklahoma Center on Aging/Center for Geroscience and Healthy Brain Aging, Department of Biochemistry and Molecular Biology, University of Oklahoma Health Sciences Center, Oklahoma City, OK, USA

Á. Nyúl-Tóth
International Training Program in Geroscience, Institute of Biophysics, Biological Research Centre, Szeged, Hungary

S. Tarantini · P. Toth · A. Tarantini · Z. Ungvari
International Training Program in Geroscience, Doctoral School of Basic and Translational Medicine/Department of Public Health, Semmelweis University, Budapest, Hungary

T. Kiss · A. Csiszar · Z. Ungvari
International Training Program in Geroscience, Theoretical Medicine Doctoral School/Departments of Medical Physics and Informatics & Cell Biology and Molecular Medicine, University of Szeged, Szeged, Hungary

P. Toth
International Training Program in Geroscience, Doctoral School of Clinical Medicine, Department of Neurosurgery and Szentagothai Research Center, Medical School, University of

Pecs, Pecs, Hungary

V. Galvan
Department of Cellular and Integrative Physiology, University of Texas Health Science Center at San Antonio, San Antonio, TX, USA

V. Galvan
Barshop Institute for Longevity and Aging Studies, University of Texas Health Science Center at San Antonio, San Antonio, TX, USA

V. Galvan
South Texas Veterans Health Care System, San Antonio, TX, USA

V. Galvan
Glenn Biggs Institute for Alzheimer's & Neurodegenerative Diseases, University of Texas Health Science Center at San Antonio, San Antonio, TX, USA

Z. Ungvari (✉)
Department of Biochemistry and Molecular Biology, Reynolds Oklahoma Center on Aging/Center for Geroscience and Healthy Brain Aging, University of Oklahoma Health Sciences Center, 975 NE 10th Street, BRC 1311, Oklahoma City, OK 73104, USA
e-mail: zoltan-ungvari@ouhsc.edu

the same level of hypertension led to significantly increased CMH burden and exacerbation of CMH-related gait alterations. In hypertensive TG2576 mice, CMHs were predominantly located in the cerebral cortex at the cortical-subcortical boundary, mimicking the clinical picture seen in patients with CAA. Collectively, amyloid pathologies exacerbate the effects of hypertension, promoting the genesis of CMHs, which likely contribute to their deleterious effects on cognitive function. Therapeutic strategies for prevention of CMHs that reduce blood pressure and preserve microvascular integrity are expected to exert neuroprotective effects in high-risk elderly AD patients.

Keywords Dementia · Microbleed · Arteriole · Gait dysfunction · Cerebral amyloid angiopathy

Introduction

Alzheimer's disease (AD) is the most common cause of dementia in older adults and the sixth leading cause of death in the USA. An estimated 5.8 million Americans aged 65 and older are living with AD, and this number is projected to reach 14 million by mid-century. There is growing evidence that microvascular pathologies contribute significantly to progression of cognitive impairment in AD [1–8]. Using sensitive magnetic resonance imaging techniques (e.g., T2* gradient-recall echo and susceptibility-weighted imaging MRI sequences) a number of cerebral microhemorrhages (CMHs) can be detected in brains of AD patients [9]. CMHs are small intracerebral hemorrhages (< 5 mm in humans) associated with rupture of small arterioles and capillaries. The prevalence of CMHs is 26–48% in AD patients [10–13]. AD patients often exhibit multiple CMHs [11, 14]. CMHs in AD patients are considered of emerging importance as a contributing factor to the progressive impairment of cognitive function [9, 15, 16]. CMHs have also been observed in mouse models of AD, including the TG2576 mice [9, 17–19]. Clinical and pre-clinical studies show that CMHs per se impair processing speed and cognitive function [15, 16], and promote gait disturbances [20–22]. The clinical significance of CMHs lies in the fact that they represent potentially preventable pathologies contributing to cognitive decline [9]. It has been proposed that treatments that target the pathogenesis of CMHs may effectively delay

progression of cognitive decline both in AD and vascular cognitive impairment (VCI) [9, 22].

Epidemiological studies demonstrate that in addition to AD pathologies, hypertension is also a major risk factor for the development of CMHs in older adults [9, 23, 24]. Preclinical studies extend these clinical findings, demonstrating that in rodent models of aging hypertension promotes the development of CMHs [9, 22, 25]. Hypertension is prevalent in AD patients, and it has been proposed that it plays a critical role in the progression of the disease [3, 13, 26–34]. For example, a recent Swedish study analyzing clinical records and autopsy findings demonstrated that 37% of AD patients analyzed had clinically manifest hypertension [35]. Additionally, large cross-sectional and longitudinal population-based studies consistently show that a relationship exists between hypertension and incidence and progression of clinical symptoms of AD [32, 33, 36–41]. Experimental studies also confirm that a causal link exist between hypertension and AD progression [3, 27, 28, 42–53]. Yet, the effects of amyloid pathologies on the on the pathogenesis of CMHs are not completely understood.

The present study was designed to test the hypothesis that the presence of amyloid pathologies exacerbates the development of hypertension-induced CMHs and aggravates their functional consequences. To test our hypothesis, we induced hypertension in the TG2576 mouse model of AD and respective controls (by treatment with angiotensin II (Ang II) and the NO synthesis inhibitor L-NAME) and compared the incidence, size, localization and neurological consequences (gait alterations) of CMHs.

Methods

Experimental animals

Wild-type control C57BL/6 ($n = 6$; 12 month old) and TG2576 (strain: B6;SJL-Tg(APP^{SWE})2576Kha; $n = 6$; 12 months old) male mice were purchased from Charles River Laboratories (Wilmington, MA, USA). The TG2576 mouse model (also known as Hsiao mice, App-Swe, App-sw, APP(sw)) overexpresses a mutant form of APP (isoform 695) with the Swedish mutation (KM670/671NL) under the control of the hamster prion protein promoter, resulting in elevated levels of A β , parenchymal amyloid plaques, and vascular amyloid angiopathy associated with cognitive impairment by 12 months of age. Animals were housed under specific

pathogen-free barrier conditions in the Rodent Barrier Facility at the University of Oklahoma Health Sciences Center with unlimited access to water under a controlled photoperiod (12 h light; 12 h dark). All procedures were approved by and followed the guidelines of the Institutional Animal Care and Use Committee of the University of Oklahoma HSC.

Induction of spontaneous CMHs

To study the effects of amyloid pathologies on spontaneous, hypertension-induced CMHs, we used a previously well-characterized mouse model [22, 25, 54–56]. Briefly, in 12-month-old male TG2576 and respective age-matched control mice hypertension was induced by a combination treatment with ω -nitro-L-arginine-methyl ether (L-NAME, 100 mg/kg/day, in drinking water) and administration of Ang-II (s.c. via osmotic mini-pumps (Alzet Model 2006, 0.15 μ l/h; Durect Co, Cupertino, CA)). Pumps were filled either with saline or solutions of angiotensin II (Sigma Chemical Co., St. Louis, MO, USA) that delivered (subcutaneously) 1 μ g/min/kg of angiotensin II. Pumps were placed into the subcutaneous space of ketamine/xylazine anesthetized mice through a small incision in the interscapular area that was closed with surgical sutures using aseptic techniques. All incision sites healed rapidly without the need for additional medication.

Blood pressure of the animals was recorded before the treatment and every second day during the treatment period using a tail-cuff blood pressure apparatus (CODA Non-Invasive Blood Pressure System, Kent Scientific Co., Torrington, CT), as described [22, 57]. To assess the occurrence of clinically manifest hemorrhages, daily neurological examination was performed as reported [22], by assessing each animal's spontaneous activity, symmetry in the movement of the four limbs, forelimb outstretching, climbing ability, body proprioception, response to vibrissae touch and gait coordination. Each examined animal was provided with a daily score calculated by the summation of all individual test scores. Animals were euthanized on day 10 post-induction of hypertension.

Analysis of gait function

To determine the impact of CMHs on gait function and the spatial and temporal aspects of interlimb coordination, we tested hypertensive control and TG2576 mice

using a highly sensitive, automated computer-assisted method (CatWalk; Noldus Information Technology Inc.) as reported [22, 57]. The CatWalk system is a sophisticated apparatus that allows for quantitative assessment of footfall and motor performance. Mouse paw location and placement patterns are recorded by a high-speed high-resolution camera while the animals are allowed to freely walk on an illuminated glass platform, providing accurate and repeatable measurements of gait function and spatial and temporal aspects of interlimb coordination [58]. Briefly, animals from both groups were acclimatized and trained to voluntarily walk across the illuminated walkway in a dark and quiet room dedicated for behavioral experimentation. Mice gait function was acquired for over 20 consecutive runs, producing over 200 steps for each animal. The resulting data was averaged across the \sim 20 runs in which mice maintained a relatively constant speed across the walkway. Subsequently, computer-aided analysis of the gait data and manual paw identification and labeling of each footprint was carried out blindly and spatial and temporal gait parameters were calculated. The variability of the data has been assessed using quartile dispersion. We adopted a common outlier definition, labeling points more than 1.5 interquartile ranges away from the sample median as extreme values. Mean gait characteristics calculated included speed, swing speed, cadence, stride length, stride time, duty cycle, base of support, and terminal dual stance. Stride length is the distance (in cm) between successive placements of the same paw. Stride time is the interval lapsed (s) between each successive paw contact. Base of support is the average width between the paws. Phase dispersion is a measure of the temporal relationship between placement of two hind paws within a step cycle. Variability characteristics and measures of gait coordination were also acquired using the CatWalk system. We also analyzed step sequence patterns. Rodents can potentially alternate between multiple step sequence patterns during spontaneous walk. The CatWalk system records the actual order of footfalls as they occur and categorizes them based on common and uncommon sequence patterns. The 4 most commonly used gait patterns in rodents, known as the “normal step patterns,” are the alternate patterns AA (RF-RH-LF-LH) and AB (LF-RH-RF-LH), and the cruciate patterns CA (RF-LF-RH-LH) and CB (LF-RF-LH-RH). To define the pattern utilized by each mouse the right front paw was arbitrarily chosen as the initial step.

The regularity index (%) is a fractional measure of inter-paw coordination, which expresses the number of normal step sequence patterns relative to the total number of paw placements.

Regularity index

$$= \frac{\text{\#of normal step sequence patterns} \times 4}{\text{total\#of paw placements}} \times (100\%)$$

In healthy, fully coordinated mice, the regularity index value is closer to 100%.

Investigating gait variability, the stride-to-stride fluctuations in gait parameters, offers a sensitive, novel method of quantifying subtle changes in locomotion in mice [58]. Step time and step length variability were analyzed by computing the standard deviation for datasets that contained > 200 steps for each animal, obtained in consecutive runs at similar speeds.

Analysis of gait symmetry provides an additional approach in the characterization of gait coordination. Importantly, as location of CMHs is asymmetric, it can be expected that assessment of gait symmetry can reveal sub-clinical alterations in gait coordination. This study investigated the effects of CMHs on gait symmetry by quantifying the symmetry index (SI). The SI is a very sensitive and commonly used assessment of gait symmetry on the basis of spatial-temporal gait characteristics [59, 60].

$$\text{Symmetry Index} = \frac{|X_{\text{Left}} - X_{\text{Right}}|}{0.5 \times (X_{\text{Left}} + X_{\text{Right}})} \times (100\%)$$

The symmetry index is a method of percentage assessment of the relative inter-limb differences between the kinematic and kinetic parameters during locomotion. The value of SI = 0 indicates full symmetry, while SI ≥ 100% indicates lack of symmetry in the gait characteristic of interest.

Histological analysis of CMHs

Mice were anesthetized and transcardially perfused with ice-cold heparinized PBS for 10 min and subsequently decapitated as reported [22]. Then, the brains were removed from the skull and fixed in 10% formalin at room temperature for 1 day. The next day, the brains were placed in fresh 10% formalin (at 4 °C, for 2 days), then in 70% ethanol (at 4 °C, for 2 days), followed by embedding in paraffin. The brains were serially sectioned at 8-μm thickness yielding approximately 1500

sections per brain. The sections were stained with hematoxylin to reveal the brain structure and diaminobenzidine (DAB) to highlight the presence of hemorrhages. DAB turns into dark brown when it undergoes a reaction with peroxidases present in red blood cells therefore allowing precise detection of extravasated blood cells in the parenchyma of the brain. All stained sections were screened by a reader blinded to the treatment groups and images were acquired in the evidence of a positive DAB reaction. Digital images were analyzed with ImageJ 1.52p (NIH, USA) software to identify the location and quantify the number and size of hemorrhages. Images captured with same magnification were color deconvolved and thresholded uniformly; then, the pixel intensity integrated density was measured on the selected bleed area. The volumetric reconstruction of individual hemorrhages was estimated based on the sum of CMH volumes on consecutive sections (CMH area x slice thickness) as described [22, 25].

Statistical analysis

Two-tailed *t* test was used for comparison of two groups. Two-way analysis of variance followed by Fisher LSD method or Kruskal-Wallis one-way analysis of variance on ranks was used for comparison of multiple groups. A *P* value < 0.05 was considered statistically significant. Data are expressed as mean ± SEM.

Results

Exacerbation of hypertension-induced spontaneous CMHs in TG2576 mice

Treatment with Ang II plus L-NAME resulted in comparable increases in blood pressure (to) both in TG2576 mice (155 ± 3 mmHg) and age-matched control (156 ± 3 mmHg) mice, extending previous findings [61]. Since aging is associated with increased activity of the vascular renin-angiotensin system and Ang II-dependent hypertension is common among older individuals, Ang II-dependent hypertension is a clinically highly relevant model to study aging-related cerebrovascular alterations [62]. Earlier studies by the Heistad laboratory [54, 55] and subsequent studies by our laboratories [22, 25] have characterized models of spontaneous hypertension-induced hemorrhages in mice. These studies showed that co-administration of L-NAME results in a ~

15 mmHg additional increase in blood pressure, which associate with a significant increase in CMH incidence in the presence of underlying microvascular fragility.

Histological analysis showed that hypertensive TG2576 mice developed multiple CMHs. CMHs varied in appearance (representative images of pericapillary, diffuse, confluent, and patchy CMHs are shown in Fig. 1). When the cerebral vessels associated with the CMHs were clearly distinguishable, their internal diameter was found to be in the range of ~ 8 – $20 \mu\text{m}$ (Fig. 1). Similar to our previous observations [57], hypertension-induced CMHs were often confined to and spread along the perivascular spaces (Fig. 1d). In brains of hypertensive TG2576 mice, a higher total count of CMHs (104 ± 14) was observed compared to hypertensive control mice (21 ± 1 ; Fig. 1f). CMHs were not detected in brains of normotensive control mice, whereas only a few small CMHs were observed in the brains of normotensive TG2576 mice (not shown).

CMHs were distributed widely in the brain of TG2576 mice, including the cortex, brain stem, basal ganglia, white matter, and even hippocampi (Fig. 2). As shown in Fig. 2b, in hypertensive TG2576 mice, there were more CMHs predominantly in cerebral cortex than in hypertensive control mice. The number of CMHs in the white matter, basal ganglia, brain stem, cerebellum, and hippocampi also increased in hypertensive TG2576 mice. CMH burden, expressed as total CMH volume in each brain region, also significantly increased in TG2576 mice (Fig. 2c). The average volume of individual CMHs was comparable in control and TG2576 animals (Fig. 2d). Figure 3 illustrates that the cortical-subcortical boundary is the predilection site of hypertension-induced CMHs in TG2576 mice. Interestingly, in human AD patients CMHs are also predominantly localized to the cortical-subcortical boundary in cortical gyri.

Increased incidence of CMHs is associated with gait dysfunction in TG2576 mice

Since in humans CMHs are associated with gait dysfunction [20], we analyzed mouse gait. We found that gait abnormalities (including an increase in gait variability and a decline in gait symmetry; Figs. 4 and 5, respectively) were more severe in hypertensive TG2576 mice as compared to hypertensive control mice, suggesting that analysis of motor function status (e.g., deficit in interlimb coordination, temporal

asymmetry) can predict the severity of CMH burden [22]. The regularity index, a comprehensive measure of inter-paw coordination, tended to be lower in hypertensive TG2576 mice as compared to hypertensive controls, but the difference did not reach statistical significance (Fig. 4a). The study of gait variability, the stride-to-stride fluctuations in walking, offers a sensitive method of quantifying and characterizing locomotion. Previous studies in older adults suggest that measures of gait variability are more closely related to cognitive decline or falls than other measures based on the mean values of other gait characteristics [63–72]. In this study, in hypertensive TG2576 mice, a trend for increased stride length variability was discernible (Fig. 4b). We found a statistically significant increase in stride time variability with advanced aging (Fig. 4c). Hypertension-induced changes in stride time and stride length (data not shown), base of support (Fig. 4d), and print area variability (Fig. 4e) did not correlate with amyloid pathology. Phase dispersion tended to change more in hypertensive TG2576 mice as compared to hypertensive controls, but the difference did not reach statistical significance (Fig. 4f, g). Gait parameters in normotensive TG2576 mice and control mice did not change significantly during the experimental period (data not shown). We found differences in the gait-pattern frequency distribution (Fig. 4h). Hypertensive TG2576 mice exhibited a 60% decrease in frequency of the radial pattern AA, known as the “giraffe walk.” Alternating contralateral footfall patterns (CA/CB) were used with similar frequency in hypertensive TG2576 mice and control mice. Thus, the changes in gait mechanics associated with increased CMH incidence in TG2576 mice, observed via gait-pattern frequency distribution, revealed that CMHs were accompanied by a preferential reliance on the AB gait pattern.

Gait involves a cyclical and laterally alternating stride progression to maintain balance. Comparing left vs right stride lengths and stride time asymmetries in hypertensive mice reflects potential functional deficits caused by asymmetric CMHs that may otherwise go unnoticed. The left-right stride characteristics were compared by calculating the symmetry indices [59] for front and hind limb stride length, stride time and paw print areas in hypertensive TG2576 mice and control mice (Fig. 5). We found that in hypertensive TG2576 mice have a more asymmetric stride pattern during gait compared to controls and tend to exhibit increased asymmetry both in stride time and stride length (Fig. 5).

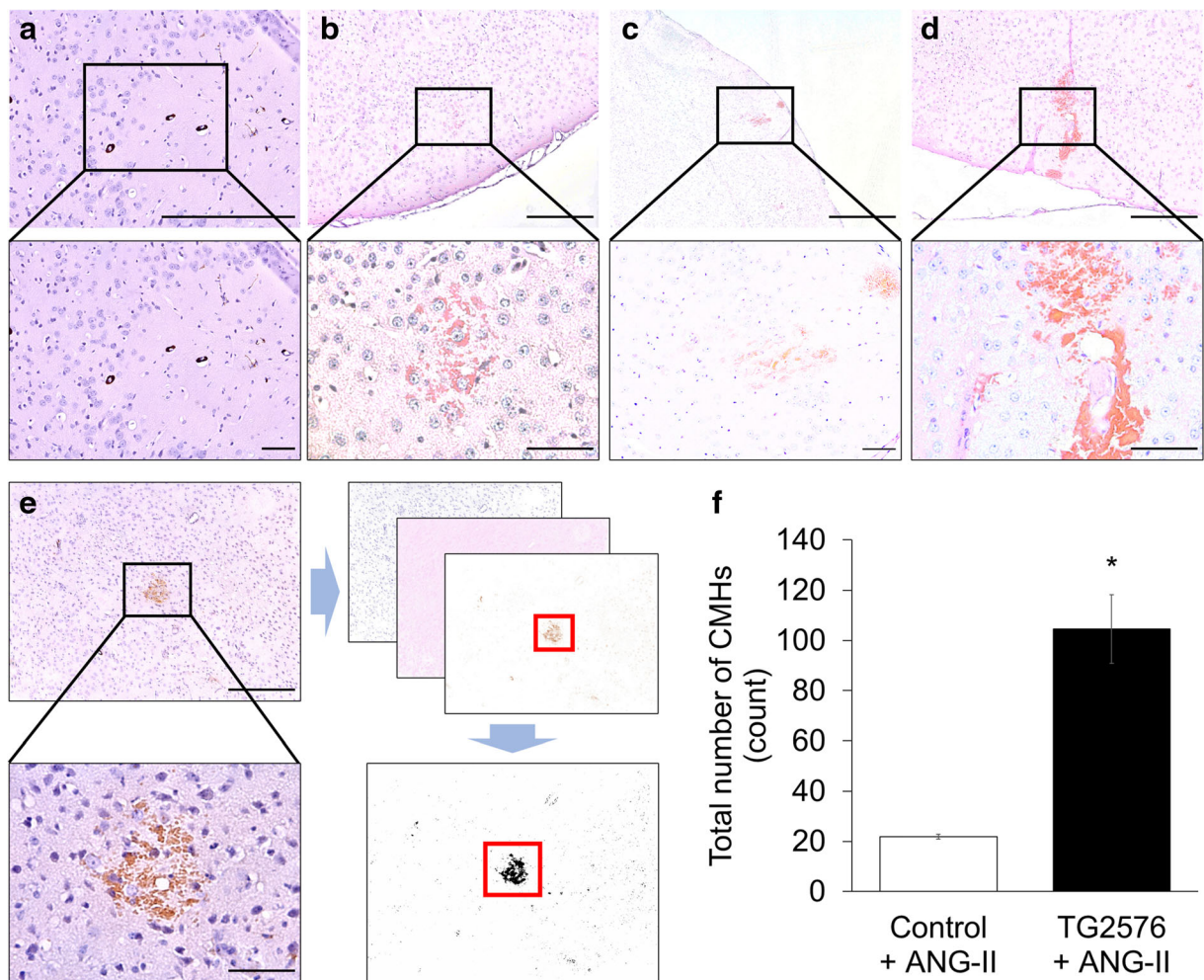


Fig. 1 Exacerbation of hypertension-induced spontaneous CMHs in TG2576 mice. Representative images of pericapillary (a), diffuse (b), patchy (c), patchy/perivasculature (d), and confluent (e) CMHs stained by diaminobenzidine in brains of hypertensive TG2576 mice (scale bar is 200 μm in case of upper panels and for lower panels is 50 μm). Note in d the spread of the hemorrhage to the daughter branches of an arteriole along the perivasculature

spaces. **e** Workflow showing analysis of CMHs. Brightfield images of CMHs were captured using a $\times 4$ objective. The images were batch-processed for color deconvolution, thresholding and area measurement. **f** Total number of hypertension (angiotensin II (Ang II) treatment)-induced CMHs throughout the entire brains of control and TG2576 mice. Data are means \pm SEM ($n = 6$ for each group). * $p < 0.0001$ vs. wild type

Discussion

Our study demonstrates that the effects of hypertension in the TG2576 mouse model of AD phenocopies important aspects of CMHs in AD patients. Our findings provide additional experimental evidence for a direct interaction between amyloid pathology and arterial hypertension in the pathogenesis of CMHs.

The majority of AD patients have cerebral amyloid angiopathy (CAA). CAA is a common age-related cerebrovascular pathology caused by the deposition of amyloid beta ($A\beta$) peptides in the cerebral arteries,

arterioles, and capillaries. The TG2576 mouse model is known to develop amyloid pathologies in cerebral vessels [73], mimicking CAA associated with AD in humans. Importantly, we found that in brains of TG2576 mice affected by amyloid pathologies, the same level of hypertension leads to significantly increased incidence of CMHs. Our findings accord with the results of the studies by Passos et al.⁶¹ reporting earlier manifestations of clinical signs of intracerebral hemorrhages upon induction of experimental hypertension in TG2576 mice as compared to control mice. The results obtained using angiotensin II-induced

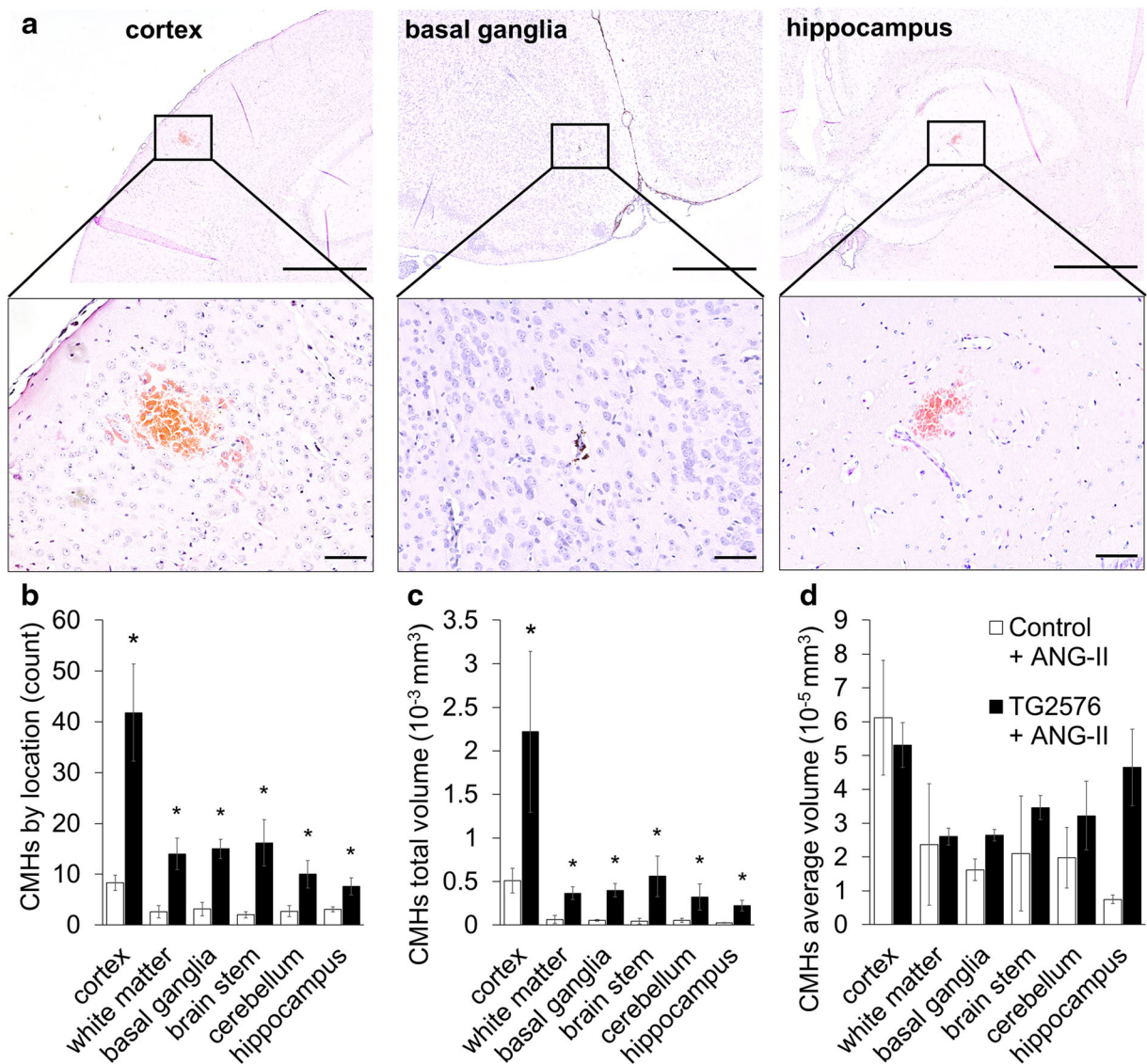


Fig. 2 Distribution of hypertension-induced CMHs by location in TG2576 mice. **a** Representative images of CMHs stained by diaminobenzidine in the cortex (left), basal ganglia (middle), and hippocampus (right) of hypertensive TG2576 mice (scale bar is 200 μm in case of upper panels and for lower panels is 50 μm). **b**, **c** Bar graphs showing the distribution of hypertension (angiotensin II (Ang II) treatment)-induced CMHs by location. Total CMH

counts (**b**) and total CMH volumes (**c**) per region per animals were averaged. Note that amyloid pathologies exacerbate hypertension-induced CMHs predominantly in the cortex. **d** Average individual CMH volumes did not differ substantially between the two groups. Data are mean \pm SEM ($n = 6$ for each group). * $p < 0.05$ vs. wild type control

hypertension as a model system have translational relevance, as in clinical studies treatment with the angiotensin-converting enzyme inhibitor perindopril to reduce blood pressure was shown to significantly reduce the risk of CAA-related CMHs [74]. We found that extravasated blood in the mouse brain often spread along the perivascular spaces. This is significant, as extravasated blood and hemosiderin were also reported

to migrate through enlarged perivascular spaces in humans propagating an inflammatory reaction along the local microvasculature [75]. We found that similar to human AD [1, 10, 76], in mice synergy of amyloid pathologies and hypertension predominantly increases the incidence of CMHs at the cortical-subcortical boundary. CAA in AD patients shows a similar distribution [77], and it is believed that majority of CMHs in

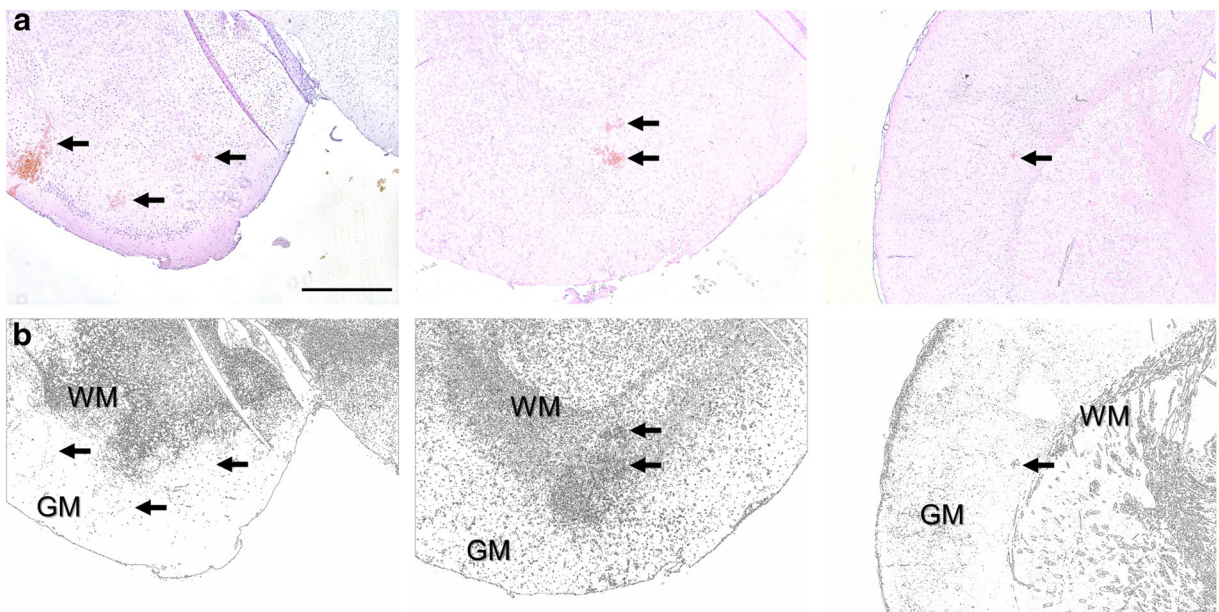


Fig. 3 The cortical-subcortical boundary is the predilection site of hypertension-induced CMHs in TG2576 mice. **a** Representative images of diaminobenzidine-stained CMHs (arrows) at the boundary between the gray matter (GM) and white matter (WM) (scale bar 500 μ m). **b** Image processing (color deconvolution followed

by thresholding) readily reveals the boundary between GM and WM on histological sections. Arrows point to the same CMHs identified in **a**. Note that both cortical and white matter CMHs are frequently located close to the cortical-subcortical boundary in brains of TG2576 mice

AD patients develop in vessels affected by CAA. Accordingly, in humans, more than 4/5 of CMHs located strictly in the lobar regions and predominantly in the posterior cortex of the brain are caused by CAA. In contrast, CMHs caused by hypertension in the absence of amyloid pathologies predominantly occur in deep gray matter or the brainstem.

The interrelationship between the location of cerebral microhemorrhages and cognitive dysfunction in humans has been studied by analyzing longitudinal data from the AGES-Reykjavik Study [78]. This study demonstrated that presence of deep or mixed (deep and lobar) CMHs in older adults is significantly associated with a steeper 5-year decline in performance on each of the following cognitive domains: memory, information processing speed, and executive function [78]. Mixed CMHs were shown to associate with a decline in memory and speed. In contrast, presence of strictly lobar CMHs or cerebellar CMHs was not associated with cognitive decline [78]. Other studies contradict the conclusions of the aforementioned study suggesting that strictly lobar, but not deep or infratentorial, CMHs are associated with cognitive impairment. Future studies should determine how number and location of CMHs in mice affect cognitive function, such as performance of commonly used cognitive tasks.

It is likely that CAA both in humans and mice increases fragility of cerebral microvessels, which become significantly more vulnerable to pressure-induced rupture. Increased microvascular fragility associated with CAA is likely also responsible for the increased prevalence of spontaneous CMHs in TG2576 mice [18, 79]. The cellular mechanisms responsible for increased susceptibility of the cerebral circulation affected by amyloid pathologies to hypertension-induced injury are likely multifaceted. Amyloid pathologies and CAA result in vascular smooth muscle cell damage, oxidative stress and matrix metalloproteinase activation, and consequential degeneration of the extracellular matrix [9, 80, 81]. High levels of A β were suggested to promote upregulation of NAD(P)H oxidase activation [82], induce mitochondrial oxidative stress, [83] and compromise antioxidant defenses [84]. Hypertension and Ang II were shown to exert synergistic vascular effects [22, 46, 85, 86]. Previous studies suggest a central role for hypertension-induced cerebrovascular ROS production and redox-sensitive activation of MMPs in the pathogenesis of CMHs [22], which degrade components of the basal lamina and extracellular matrix, weakening the vascular wall. Amyloid pathologies in TG2576 mice are associated with increased MMP activation/expression

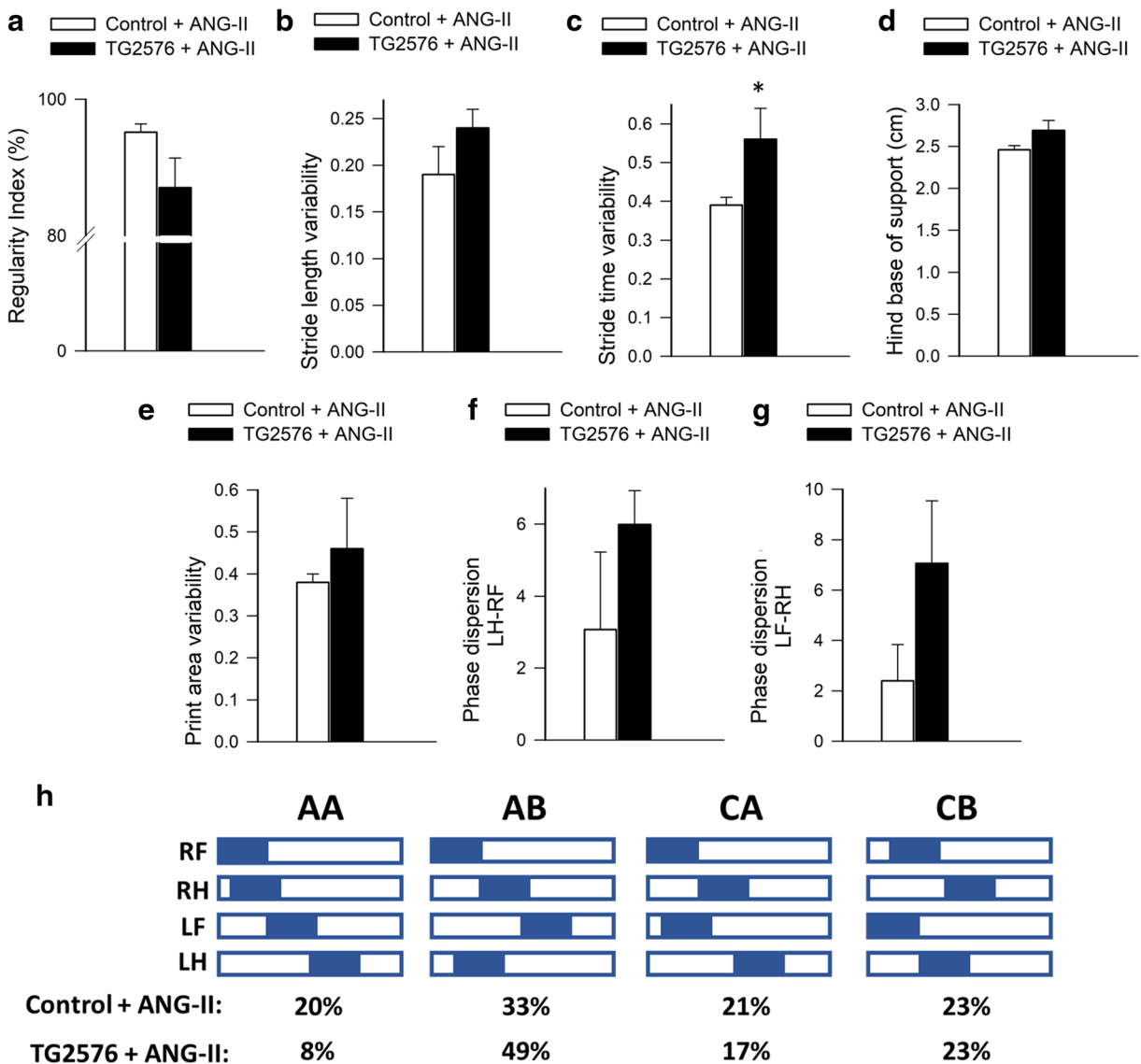


Fig. 4 Effects of increased incidence of CMHs on gait coordination in hypertensive TG2576 mice. Regularity index (a), stride length variability (b), stride time variability (c), base of support (hind paws; d), and print area variability (e) in spontaneously walking hypertensive TG2576 mice and control mice after induction of CMHs. f, g Bar graphs showing average deviation of inter-limb coupling values (phase dispersion) from the expected value (50%) after induction of CMHs in hypertensive control mice and TG2576 mice. Phase dispersion was calculated between the right front paw (RF) and left hind paw (LH) (f) and the right hind paw

(RH) and left front paw (LF) (g). Data are mean ± SEM (n = 6 for each group). *p < 0.05 vs. control. h Hildebrand plot of the common gait patterns: AA (RF-RH-LF-LH), AB (LF-RH-RF-LH), CA (RF-LF-RH-LH), and CB (LF-RF-LH-RH). Percentages indicate relative use of each step pattern in hypertensive TG2576 mice and control mice. The most common step pattern in both was the AB pattern. Hypertensive control mice used more frequently the radial AA pattern than hypertensive TG2576 mice, and compensated with a decreased use of the alternating AB pattern

[87], which likely contribute to the increased fragility of cerebral blood vessels. Treatment with Aβ peptide in vitro also upregulates MMPs [81]. Additionally, amyloid pathologies exacerbate cerebrovascular oxidative stress [88], presenting redox-sensitive MMP activation

[54] as a potential mechanism responsible for the observed phenotype. This concept is supported by previous findings that hypertension-induced MMP activation can be attenuated by antioxidant treatments [22]. Future studies are warranted to determine the effects of

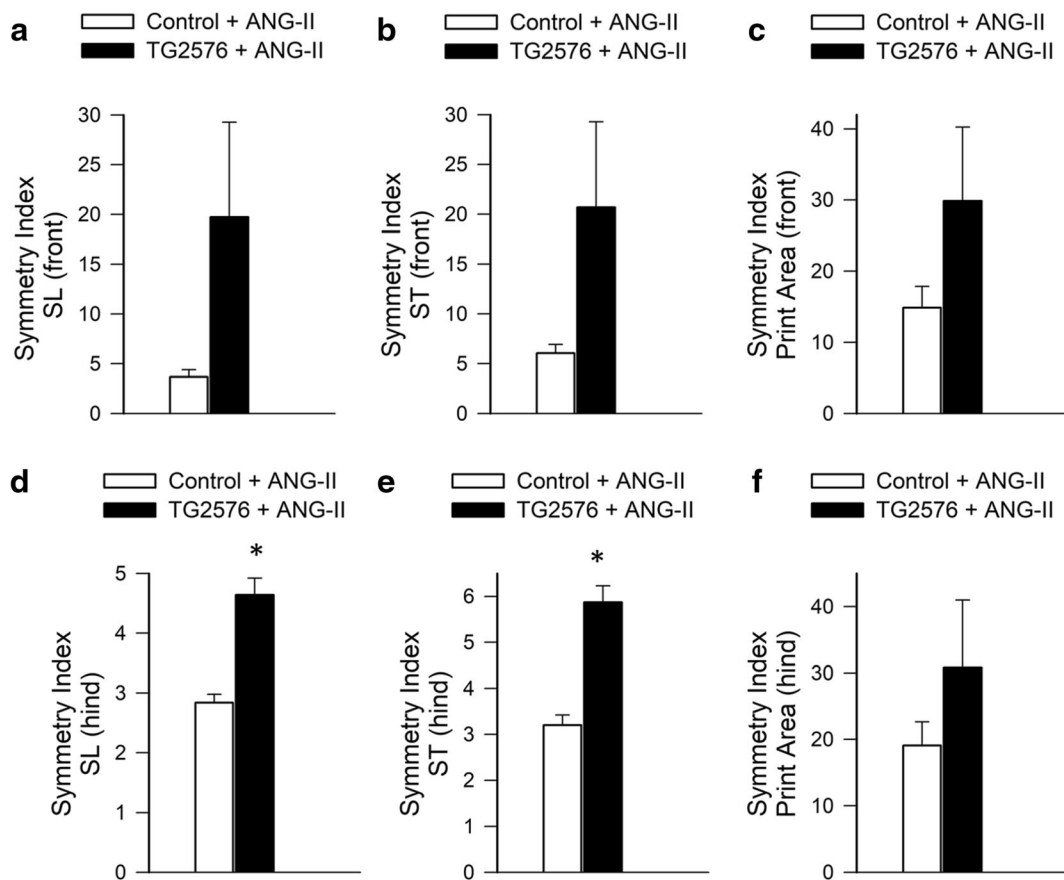


Fig. 5 Effects of increased incidence of CMHs on gait symmetry in hypertensive TG2576 mice. Gait symmetry indices were calculated to analyze the relationship between left and right stride lengths (SL), stride times (ST), and paw print areas of front and

hind limbs. Bar graphs depict symmetry indices for front and hind limb SL (**a, d**), ST (**b, e**), and paw print areas (**c, f**), respectively, in hypertensive TG2576 mice and control mice. Data are mean \pm SEM ($n = 6$ for each group). * $p < 0.05$ vs. control

antioxidants and MMP inhibitors on the genesis of hypertension-induced CMHs in AD as well.

Our findings underscore the likely pathogenic role of hypertension-induced CMHs in AD patients. Indeed, there are many similarities between CMHs observed in TG2576 mice and hypertensive elderly AD patients, including the relative size of the bleedings, the clinical symptoms, and the progressive nature of the pathological process [61, 89]. Clinical studies show that CMHs contribute to the pathogenesis of cognitive impairment [90]. Additionally, CMHs have also been shown to be associated with gait dysfunction both in humans [20] and experimental animals [22, 25]. Importantly, we also revealed that increased incidence of CMHs lead to progressive gait abnormalities in TG2576 mice. Gait is a complex motor behavior which involves all levels of the nervous system from cortex to brain stem that coordinate to produce locomotion. We propose that subclinical

gait abnormalities are sensitive indicators of CMH development in experimental AD research as lesions affecting brain regions important for gait coordination (e.g., multiple cortical areas, basal ganglia, cerebellum, white matter) will elicit quantifiable symptoms. The causal link between CMHs and gait abnormalities is clinically potentially significant as gait abnormalities are early signs of AD and dementia in humans [91–93].

In conclusion, our results add to the growing evidence that hypertension exacerbates the progression of cognitive decline in AD patients, at least in part, by promoting the development of CMHs. Additional mechanisms by which hypertension may impair cognitive function in AD patients include induction of capillary rarefaction [94], neurovascular uncoupling [27, 31, 45, 46, 95, 96], blood-brain barrier disruption [62], neuroinflammation, and synaptic dysfunction. Further, hypertension also exacerbates amyloid pathologies. For

example, in mice co-expressing KM670/671NL Swedish mutated amyloid precursor protein and the Leu to Pro mutated presenilin-1 (APPS1) administration of hypertensive dose of angiotensin II was reported to associate with exacerbated amyloid pathology, capillary damage and increased cognitive deficit [43]. Other studies showed that angiotensin II-induced hypertension increases microvascular amyloid deposition in the TG2576 mice [27, 51]. Hypertension induced by transverse aortic coarctation was also reported to exacerbate A β -deposition in the mouse brain, promoting cognitive decline [48–50]. Our findings, taken together with the results of earlier studies [17, 18, 22, 61, 74, 97], point to potential benefits of interventions normalizing blood pressure and promoting microvascular health for prevention of CMHs and cognitive decline in older AD patients. Importantly, microvascular-targeted treatments that are effective for prevention of CMHs may also improve microvascular vasodilator and barrier functions [62], contributing to a broad-range neuroprotective strategy.

Funding information This work was supported by grants from the American Heart Association (ST), the Oklahoma Center for the Advancement of Science and Technology (to AC, AY, ZU), the National Institute on Aging (R01-AG047879; R01-AG038747; R01-AG055395), the National Institute of Neurological Disorders and Stroke (NINDS; R01-NS056218 to AC, R01-NS100782 to ZU), the National Institute of General Medical Sciences Oklahoma Shared Clinical and Translational Resources (OSCTR) (GM104938, to AY), the Presbyterian Health Foundation (to ZU, AC, AY), the NIA-supported Geroscience Training Program in Oklahoma (T32AG052363), the Oklahoma Nathan Shock Center (P30AG050911), and the Cellular and Molecular GeroScience CoBRE (1P20GM125528, sub#5337). The funding sources had no role in the study design; in the collection, analysis, and interpretation of data; in the writing of the report; and in the decision to submit the article for publication.

Compliance with ethical standards

Conflict of interest The authors declare that they have no conflict of interest.

References

- Gorelick PB, Scuteri A, Black SE, Decarli C, Greenberg SM, Iadecola C, et al. Vascular contributions to cognitive impairment and dementia: a statement for healthcare professionals from the American Heart Association/American Stroke Association. *Stroke*. 2011;42:2672–713.
- Iadecola C, Gottesman RF. Cerebrovascular alterations in Alzheimer disease. *Circ Res*. 2018;123:406–8.
- Iadecola C, Park L, Capone C. Threats to the mind: aging, amyloid, and hypertension. *Stroke*. 2009;40:S40–4.
- Kisler K, Nelson AR, Montagne A, Zlokovic BV. Cerebral blood flow regulation and neurovascular dysfunction in Alzheimer disease. *Nat Rev Neurosci*. 2017;18:419–34.
- Sweeney MD, Sagare AP, Zlokovic BV. Blood-brain barrier breakdown in Alzheimer disease and other neurodegenerative disorders. *Nat Rev Neurol*. 2018;14:133–50.
- Tarantini S, Tran CHT, Gordon GR, Ungvari Z, Csiszar A. Impaired neurovascular coupling in aging and Alzheimer's disease: contribution of astrocyte dysfunction and endothelial impairment to cognitive decline. *Exp Gerontol*. 2017;94:52–8.
- Toth P, Tarantini S, Csiszar A, Ungvari Z. Functional vascular contributions to cognitive impairment and dementia: mechanisms and consequences of cerebral autoregulatory dysfunction, endothelial impairment, and neurovascular uncoupling in aging. *Am J Physiol Heart Circ Physiol*. 2017;312:H1–H20.
- Van Skike CE, Jahrling JB, Olson AB, Sayre NL, Hussong SA, Ungvari Z, et al. Inhibition of mTOR protects the blood-brain barrier in models of Alzheimer's disease and vascular cognitive impairment. *Am J Physiol Heart Circ Physiol*. 2018;314:H693–703.
- Ungvari Z, Tarantini S, Kirkpatrick AC, Csiszar A, Prodan CI. Cerebral microhemorrhages: mechanisms, consequences, and prevention. *Am J Physiol Heart Circ Physiol*. 2017;312:H1128–43.
- Yates PA, Sirisriro R, Villemagne VL, Farquharson S, Masters CL, Rowe CC. Cerebral microhemorrhage and brain beta-amyloid in aging and Alzheimer disease. *Neurology*. 2011;77:48–54.
- Pettersen JA, Sathiyamoorthy G, Gao FQ, Szilagyi G, Nadkarni NK, St George-Hyslop P, et al. Microbleed topography, leukoaraiosis, and cognition in probable Alzheimer disease from the Sunnybrook dementia study. *Arch Neurol*. 2008;65:790–5.
- Yates PA, Desmond PM, Phal PM, Steward C, Szoek C, Salvado O, et al. Incidence of cerebral microbleeds in preclinical Alzheimer disease. *Neurology*. 2014;82:1266–73.
- Benedictus MR, Goos JD, Binnewijzend MA, Muller M, Barkhof F, Scheltens P, et al. Specific risk factors for microbleeds and white matter hyperintensities in Alzheimer's disease. *Neurobiol Aging*. 2013;34:2488–94.
- Goos JD, Kester MI, Barkhof F, Klein M, Blankenstein MA, Scheltens P, et al. Patients with Alzheimer disease with multiple microbleeds: relation with cerebrospinal fluid biomarkers and cognition. *Stroke*. 2009;40:3455–60.
- Akoudad S, Wolters FJ, Viswanathan A, de Bruijn RF, van der Lugt A, Hofman A, et al. Association of cerebral microbleeds with cognitive decline and dementia. *JAMA Neurol*. 2016;73:934–43.
- Poels MM, Ikram MA, van der Lugt A, Hofman A, Niessen WJ, Krestin GP, et al. Cerebral microbleeds are associated with worse cognitive function: the Rotterdam Scan Study. *Neurology*. 2012;78:326–33.
- Han BH, Zhou ML, Johnson AW, Singh I, Liao F, Vellimana AK, et al. Contribution of reactive oxygen species to cerebral amyloid angiopathy, vasomotor dysfunction,

- and microhemorrhage in aged Tg2576 mice. *Proc Natl Acad Sci U S A*. 2015;112:E881–90.
18. Hur J, Mateo V, Amalric N, Babiak M, Bereziat G, Kanony-Truc C, et al. Cerebrovascular beta-amyloid deposition and associated microhemorrhages in a Tg2576 Alzheimer mouse model are reduced with a DHA-enriched diet. *FASEB J*. 2018;32:4972–83.
 19. Fisher M, Vasilevko V, Passos GF, Ventura C, Quiring D, Cribbs DH. Therapeutic modulation of cerebral microhemorrhage in a mouse model of cerebral amyloid angiopathy. *Stroke*. 2011;42:3300–3.
 20. Choi P, Ren M, Phan TG, Callisaya M, Ly JV, Beare R, et al. Silent infarcts and cerebral microbleeds modify the associations of white matter lesions with gait and postural stability: population-based study. *Stroke*. 2012;43:1505–10.
 21. de Laat KF, van den Berg HA, van Norden AG, Gons RA, Olde Rikkert MG, de Leeuw FE. Microbleeds are independently related to gait disturbances in elderly individuals with cerebral small vessel disease. *Stroke*. 2011;42:494–7.
 22. Toth P, Tarantini S, Springo Z, Tucsek Z, Gautam T, Giles CB, et al. Aging exacerbates hypertension-induced cerebral microhemorrhages in mice: role of resveratrol treatment in vasoprotection. *Aging Cell*. 2015;14:400–8.
 23. Poels MM, Ikram MA, van der Lugt A, Hofman A, Krestin GP, Breteler MM, et al. Incidence of cerebral microbleeds in the general population: the Rotterdam Scan Study. *Stroke*. 2011;42:656–61.
 24. Kato H, Izumiyama M, Izumiyama K, Takahashi A, Itoyama Y. Silent cerebral microbleeds on T2*-weighted MRI: correlation with stroke subtype, stroke recurrence, and leukoaraiosis. *Stroke*. 2002;33:1536–40.
 25. Tarantini S, Valcarcel-Ares NM, Yabluchanskiy A, Springo Z, Fulop GA, Ashpole N, et al. Insulin-like growth factor 1 deficiency exacerbates hypertension-induced cerebral microhemorrhages in mice, mimicking the aging phenotype. *Aging Cell*. 2017;16:469–79.
 26. Barthold D, Joyce G, Wharton W, Kehoe P, Zissimopoulos J. The association of multiple anti-hypertensive medication classes with Alzheimer's disease incidence across sex, race, and ethnicity. *PLoS One*. 2018;13:e0206705.
 27. Faraco G, Park L, Zhou P, Luo W, Paul SM, Anrather J, et al. Hypertension enhances Abeta-induced neurovascular dysfunction, promotes beta-secretase activity, and leads to amyloidogenic processing of APP. *J Cereb Blood Flow Metab*. 2016;36:241–52.
 28. Farkas E, De Jong GI, Apro E, De Vos RA, Steur EN, Luiten PG. Similar ultrastructural breakdown of cerebrocortical capillaries in Alzheimer's disease, Parkinson's disease, and experimental hypertension. What is the functional link? *Ann N Y Acad Sci*. 2000;903:72–82.
 29. Hoffman LB, Schmeidler J, Lesser GT, Beeri MS, Purohit DP, Grossman HT, et al. Less Alzheimer disease neuropathology in medicated hypertensive than nonhypertensive persons. *Neurology*. 2009;72:1720–6.
 30. Iadecola C. Hypertension and dementia. *Hypertension*. 2014;64:3–5.
 31. Iadecola C, Yaffe K, Biller J, Bratzke LC, Faraci FM, Gorelick PB, et al. Impact of hypertension on cognitive function: a scientific statement from the American Heart Association. *Hypertension*. 2016;68:e67–94.
 32. Israeli-Korn SD, Masarwa M, Schechtman E, Abuful A, Strugatsky R, Avni S, et al. Hypertension increases the probability of Alzheimer's disease and of mild cognitive impairment in an Arab community in northern Israel. *Neuroepidemiology*. 2010;34:99–105.
 33. Launer LJ, Ross GW, Petrovitch H, Masaki K, Foley D, White LR, et al. Midlife blood pressure and dementia: the Honolulu-Asia aging study. *Neurobiol Aging*. 2000;21:49–55.
 34. Wiesmann M, Roelofs M, van der Lugt R, Heerschap A, Kiliaan AJ, Claassen JA. Angiotensin II, hypertension, and angiotensin II receptor antagonism: roles in the behavioural and brain pathology of a mouse model of Alzheimer's disease. *J Cereb Blood Flow Metab*. 2017;37(7):2396–2413. <https://doi.org/10.1177/0271678X16667364>.
 35. Javanshiri K, Waldo ML, Friberg N, Sjovald F, Wickerstrom K, Haglund M, et al. Atherosclerosis, hypertension, and diabetes in Alzheimer's disease, vascular dementia, and mixed dementia: prevalence and presentation. *J Alzheimers Dis*. 2018;65:1247–58.
 36. Forette F, Seux ML, Staessen JA, Thijs L, Birkenhager WH, Babarskiene MR, et al. Prevention of dementia in randomised double-blind placebo-controlled Systolic Hypertension in Europe (Syst-Eur) trial. *Lancet*. 1998;352:1347–51.
 37. Guo Z, Qiu C, Viitanen M, Fastbom J, Winblad B, Fratiglioni L. Blood pressure and dementia in persons 75+ years old: 3-year follow-up results from the Kungsholmen Project. *J Alzheimers Dis*. 2001;3:585–91.
 38. Marr RA, Hafez DM. Amyloid-beta and Alzheimer's disease: the role of neprilysin-2 in amyloid-beta clearance. *Front Aging Neurosci*. 2014;6:187.
 39. Petrovitch H, White LR, Izmirilian G, Ross GW, Havlik RJ, Markesbery W, et al. Midlife blood pressure and neuritic plaques, neurofibrillary tangles, and brain weight at death: the HAAS. Honolulu-Asia aging study. *Neurobiol Aging*. 2000;21:57–62.
 40. van Dijk EJ, Breteler MM, Schmidt R, Berger K, Nilsson LG, Oudkerk M, et al. The association between blood pressure, hypertension, and cerebral white matter lesions: cardiovascular determinants of dementia study. *Hypertension*. 2004;44:625–30.
 41. Joas E, Backman K, Gustafson D, Ostling S, Waern M, Guo X, et al. Blood pressure trajectories from midlife to late life in relation to dementia in women followed for 37 years. *Hypertension*. 2012;59:796–801.
 42. Cifuentes D, Poittevin M, Bonnin P, Ngkelo A, Kubis N, Merkulova-Rainon T, et al. Inactivation of nitric oxide synthesis exacerbates the development of Alzheimer disease pathology in APPPS1 mice (amyloid precursor protein/presenilin-1). *Hypertension*. 2017;70:613–23.
 43. Cifuentes D, Poittevin M, Dere E, Broqueres-You D, Bonnin P, Benessiano J, et al. Hypertension accelerates the progression of Alzheimer-like pathology in a mouse model of the disease. *Hypertension*. 2015;65:218–24.
 44. Capone C, Faraco G, Peterson JR, Coleman C, Anrather J, Milner TA, et al. Central cardiovascular circuits contribute to the neurovascular dysfunction in angiotensin II hypertension. *J Neurosci*. 2012;32:4878–86.
 45. Girouard H, Park L, Anrather J, Zhou P, Iadecola C. Angiotensin II attenuates endothelium-dependent responses

- in the cerebral microcirculation through nox-2-derived radicals. *Arterioscler Thromb Vasc Biol.* 2006;26:826–32.
46. Kazama K, Anrather J, Zhou P, Girouard H, Frys K, Milner TA, et al. Angiotensin II impairs neurovascular coupling in neocortex through NADPH oxidase-derived radicals. *Circ Res.* 2004;95:1019–26.
 47. Niwa K, Kazama K, Younkin L, Younkin SG, Carlson GA, Iadecola C. Cerebrovascular autoregulation is profoundly impaired in mice overexpressing amyloid precursor protein. *Am J Physiol Heart Circ Physiol.* 2002;283:H315–23.
 48. Carnevale D, Lembo G. ‘Alzheimer-like’ pathology in a murine model of arterial hypertension. *Biochem Soc Trans.* 2011;39:939–44.
 49. Carnevale D, Mascio G, Ajmone-Cat MA, D’Andrea I, Cifelli G, Madonna M, et al. Role of neuroinflammation in hypertension-induced brain amyloid pathology. *Neurobiol Aging.* 2012;33:205 e19–29.
 50. Carnevale D, Mascio G, D’Andrea I, Fardella V, Bell RD, Branchi I, et al. Hypertension induces brain beta-amyloid accumulation, cognitive impairment, and memory deterioration through activation of receptor for advanced glycation end products in brain vasculature. *Hypertension.* 2012;60:188–97.
 51. Diaz-Ruiz C, Wang J, Ksiezak-Reding H, Ho L, Qian X, Humala N, et al. Role of hypertension in aggravating Abeta neuropathology of AD type and tau-mediated motor impairment. *Cardiovasc Psychiatry Neurol.* 2009;2009:107286.
 52. Hsu CY, Huang CC, Chan WL, Huang PH, Chiang CH, Chen TJ, et al. Angiotensin-receptor blockers and risk of Alzheimer’s disease in hypertension population. *Circ J.* 2013;77:405–10.
 53. Sparks DL, Scheff SW, Liu H, Landers TM, Coyne CM, Hunsaker JC 3rd. Increased incidence of neurofibrillary tangles (NFT) in non-demented individuals with hypertension. *J Neurol Sci.* 1995;131:162–9.
 54. Wakisaka Y, Chu Y, Miller JD, Rosenberg GA, Heistad DD. Critical role for copper/zinc-superoxide dismutase in preventing spontaneous intracerebral hemorrhage during acute and chronic hypertension in mice. *Stroke.* 2010;41(4):790–7. <https://doi.org/10.1161/STROKEAHA.109.569616>.
 55. Wakisaka Y, Chu Y, Miller JD, Rosenberg GA, Heistad DD. Spontaneous intracerebral hemorrhage during acute and chronic hypertension in mice. *J Cereb Blood Flow Metab.* 2010;30:56–69.
 56. Wakisaka Y, Miller JD, Chu Y, Baumbach GL, Wilson S, Faraci FM, et al. Oxidative stress through activation of NAD(P)H oxidase in hypertensive mice with spontaneous intracranial hemorrhage. *J Cereb Blood Flow Metab.* 2008;28:1175–85.
 57. Tarantini S, Giles CB, Wren JD, Ashpole NM, Valcarcel-Ares MN, Wei JY, et al. IGF-1 deficiency in a critical period early in life influences the vascular aging phenotype in mice by altering miRNA-mediated post-transcriptional gene regulation: implications for the developmental origins of health and disease hypothesis. *Age (Dordr).* 2016;38:239–58.
 58. Tarantini S, Yabluchanskiy A, Fulop GA, Kiss T, Perz A, O’Connor D, et al. Age-related alterations in gait function in freely moving male C57BL/6 mice: translational relevance of decreased cadence and increased gait variability. *J Gerontol A Biol Sci Med Sci.* 2018.
 59. Blazkiewicz M, Wiszomirska I, Wit A. Comparison of four methods of calculating the symmetry of spatial-temporal parameters of gait. *Acta Bioeng Biomech.* 2014;16:29–35.
 60. Tarantini S, Yabluchanskiy A, Fulop GA, Kiss T, Perz A, O’Connor D, et al. Age-related alterations in gait function in freely moving male C57BL/6 mice: translational relevance of decreased cadence and increased gait variability. *J Gerontol A Biol Sci Med Sci.* 2019;74:1417–21.
 61. Passos GF, Kilday K, Gillen DL, Cribbs DH, Vasilevko V. Experimental hypertension increases spontaneous intracerebral hemorrhages in a mouse model of cerebral amyloidosis. *J Cereb Blood Flow Metab.* 2016;36:399–404.
 62. Toth P, Tucsek Z, Sosnowska D, Gautam T, Mitschelen M, Tarantini S, et al. Age-related autoregulatory dysfunction and cerebromicrovascular injury in mice with angiotensin II-induced hypertension. *J Cereb Blood Flow Metab.* 2013;33:1732–42.
 63. Nakamura T, Meguro K, Sasaki H. Relationship between falls and stride length variability in senile dementia of the Alzheimer type. *Gerontology.* 1996;42:108–13.
 64. Montero-Odasso M, Oteng-Amoako A, Speechley M, Gopaul K, Beauchet O, Annweiler C, et al. The motor signature of mild cognitive impairment: results from the gait and brain study. *J Gerontol A Biol Sci Med Sci.* 2014;69:1415–21.
 65. Rosso AL, Olson Hunt MJ, Yang M, Brach JS, Harris TB, Newman AB, et al. Higher step length variability indicates lower gray matter integrity of selected regions in older adults. *Gait Posture.* 2014;40:225–30.
 66. Studenski S, Perera S, Patel K, Rosano C, Faulkner K, Inzitari M, et al. Gait speed and survival in older adults. *JAMA.* 2011;305:50–8.
 67. Verghese J, Holtzer R, Lipton RB, Wang C. Quantitative gait markers and incident fall risk in older adults. *J Gerontol A Biol Sci Med Sci.* 2009;64:896–901.
 68. Verghese J, Robbins M, Holtzer R, Zimmerman M, Wang C, Xue X, et al. Gait dysfunction in mild cognitive impairment syndromes. *J Am Geriatr Soc.* 2008;56:1244–51.
 69. Verghese J, Wang C, Lipton RB, Holtzer R, Xue X. Quantitative gait dysfunction and risk of cognitive decline and dementia. *J Neurol Neurosurg Psychiatry.* 2007;78:929–35.
 70. Verlinden VJ, van der Geest JN, Hoogendam YY, Hofman A, Breteler MM, Ikram MA. Gait patterns in a community-dwelling population aged 50 years and older. *Gait Posture.* 2013;37:500–5.
 71. Visser H. Gait and balance in senile dementia of Alzheimer’s type. *Age Ageing.* 1983;12:296–301.
 72. Wittwer JE, Webster KE, Hill K. Reproducibility of gait variability measures in people with Alzheimer’s disease. *Gait Posture.* 2013;38:507–10.
 73. Manso Y, Comes G, Lopez-Ramos JC, Belfiore M, Molinero A, Giralt M, et al. Overexpression of metallothionein-1 modulates the phenotype of the Tg2576 mouse model of Alzheimer’s disease. *J Alzheimers Dis.* 2016;51:81–95.
 74. Arima H, Tzourio C, Anderson C, Woodward M, Bousser MG, MacMahon S, et al. Effects of perindopril-based lowering of blood pressure on intracerebral hemorrhage related to amyloid angiopathy: the PROGRESS trial. *Stroke.* 2010;41:394–6.

75. Schrag M, McAuley G, Pomakian J, Jiffry A, Tung S, Mueller C, et al. Correlation of hypointensities in susceptibility-weighted images to tissue histology in dementia patients with cerebral amyloid angiopathy: a postmortem MRI study. *Acta Neuropathol.* 2010;119:291–302.
76. Ni J, Auriel E, Martinez-Ramirez S, Keil B, Reed AK, Fotiadis P, et al. Cortical localization of microbleeds in cerebral amyloid angiopathy: an ultra high-field 7T MRI study. *J Alzheimers Dis.* 2015;43:1325–30.
77. Vinters HV, Gilbert JJ. Cerebral amyloid angiopathy: incidence and complications in the aging brain. II. The distribution of amyloid vascular changes. *Stroke.* 1983;14:924–8.
78. Ding J, Sigurethsson S, Jonsson PV, Eiriksdottir G, Meirelles O, Kjartansson O, et al. Space and location of cerebral microbleeds, cognitive decline, and dementia in the community. *Neurology.* 2017;88:2089–97.
79. Michael N, Grigoryan MM, Kilday K, Sumbria RK, Vasilevko V, van Ryn J, et al. Effects of dabigatran in mouse models of aging and cerebral amyloid angiopathy. *Front Neurol.* 2019;10:966.
80. Lee JM, Yin K, Hsin I, Chen S, Fryer JD, Holtzman DM, et al. Matrix metalloproteinase-9 in cerebral-amyloid-angiopathy-related hemorrhage. *J Neurol Sci.* 2005;229–230:249–54.
81. Lee JM, Yin KJ, Hsin I, Chen S, Fryer JD, Holtzman DM, et al. Matrix metalloproteinase-9 and spontaneous hemorrhage in an animal model of cerebral amyloid angiopathy. *Ann Neurol.* 2003;54:379–82.
82. Park L, Anrather J, Zhou P, Frys K, Pistick R, Younkin S, et al. NADPH-oxidase-derived reactive oxygen species mediate the cerebrovascular dysfunction induced by the amyloid beta peptide. *J Neurosci.* 2005;25:1769–77.
83. Cheignon C, Tomas M, Bonnefont-Rousselot D, Faller P, Hureau C, Collin F. Oxidative stress and the amyloid beta peptide in Alzheimer's disease. *Redox Biol.* 2018;14:450–64.
84. Sen A, Nelson TJ, Alkon DL, Hongpaisan J. Loss in PKC epsilon causes downregulation of MnSOD and BDNF expression in neurons of Alzheimer's disease Hippocampus. *J Alzheimers Dis.* 2018;63:1173–89.
85. Springo Z, Tarantini S, Toth P, Tucsek Z, Koller A, Sonntag WE, et al. Aging exacerbates pressure-induced mitochondrial oxidative stress in mouse cerebral arteries. *J Gerontol A Biol Sci Med Sci.* 2015;70:1355–9.
86. Dushpanova A, Agostini S, Ciofini E, Cabiati M, Casieri V, Matteucci M, et al. Gene silencing of endothelial von Willebrand factor attenuates angiotensin II-induced endothelin-I expression in porcine aortic endothelial cells. *Sci Rep.* 2016;6:30048.
87. Yan P, Zhu A, Liao F, Xiao Q, Kraft A, Gonzales E, et al. Minocycline reduces spontaneous hemorrhage in mouse models of cerebral amyloid angiopathy. *Stroke.* 2015;46:1633–40.
88. Park L, Uekawa K, Garcia-Bonilla L, Koizumi K, Murphy M, Pistik R, et al. Brain perivascular macrophages initiate the neurovascular dysfunction of Alzheimer Abeta peptides. *Circ Res.* 2017;121:258–69.
89. Lee SH, Lee ST, Kim BJ, Park HK, Kim CK, Jung KH, et al. Dynamic temporal change of cerebral microbleeds: long-term follow-up MRI study. *PLoS One.* 2011;6:e25930.
90. Seo SW, Hwa Lee B, Kim EJ, Chin J, Sun Cho Y, Yoon U, et al. Clinical significance of microbleeds in subcortical vascular dementia. *Stroke.* 2007;38:1949–51.
91. Bature F, Guinn BA, Pang D, Pappas Y. Signs and symptoms preceding the diagnosis of Alzheimer's disease: a systematic scoping review of literature from 1937 to 2016. *BMJ Open.* 2017;7:e015746.
92. Rucco R, Agosti V, Jacini F, Sorrentino P, Varriale P, De Stefano M, et al. Spatio-temporal and kinematic gait analysis in patients with frontotemporal dementia and Alzheimer's disease through 3D motion capture. *Gait Posture.* 2017;52:312–7.
93. Allan LM, Ballard CG, Burn DJ, Kenny RA. Prevalence and severity of gait disorders in Alzheimer's and non-Alzheimer's dementias. *J Am Geriatr Soc.* 2005;53:1681–7.
94. Tarantini S, Tucsek Z, Valcarcel-Ares M, Toth P, Gautam T, Giles C, et al. Circulating IGF-1 deficiency exacerbates hypertension-induced microvascular rarefaction in the mouse hippocampus and retrosplenial cortex: implications for cerebrovascular and brain aging. *Age (Dordr).* 2016;38:273–89.
95. Iadecola C, Gottesman RF. Neurovascular and cognitive dysfunction in hypertension. *Circ Res.* 2019;124:1025–44.
96. Kazama K, Wang G, Frys K, Anrather J, Iadecola C. Angiotensin II attenuates functional hyperemia in the mouse somatosensory cortex. *Am J Physiol Heart Circ Physiol.* 2003;285:H1890–9.
97. Lin AL, Zheng W, Halloran JJ, Burbank RR, Hussong SA, Hart MJ, et al. Chronic rapamycin restores brain vascular integrity and function through NO synthase activation and improves memory in symptomatic mice modeling Alzheimer's disease. *J Cereb Blood Flow Metab.* 2013;33:1412–21.

Publisher's note Springer Nature remains neutral with regard to jurisdictional claims in published maps and institutional affiliations.